Insulin-like Growth Factor-1 Induces an Inositol 1,4,5-Trisphosphate-dependent Increase in Nuclear and Cytosolic Calcium in Cultured Rat Cardiac Myocytes*

Cristian Ibarra‡§¶, Manuel Estrada§‖, Loreto Carrasco‡¶, Mario Chiong‡, José L. Liberona§‖, César Cardenas§‖, Guillermo Díaz-Araya, Enrique Jaimovich§‖‡‡, and Sergio Lavandero‡§‖§§**

*From the Departamentos de ‡Bioquímica y Biología Molecular y **Química Farmacológica y Toxicológica, Facultad de Ciencias Químicas y Farmacéuticas, the ‖Instituto de Ciencias Biomédicas, Facultad de Medicina, the §Centro FONDAP Estudios Moleculares de la Célula, Universidad de Chile, Santiago 6640750, Chile*

In the heart, insulin-like growth factor-1 (IGF-1) is a pro-hypertrophic and anti-apoptotic peptide. In cultured rat cardiomyocytes, IGF-1 induced a fast and transient increase in Ca^{2+}_i levels apparent both in the nucleus and cytosol, releasing this ion from intracellular stores through an inositol 1,4,5-trisphosphate (IP_3)-dependent signaling pathway. Intracellular IP_3 levels increased after IGF-1 stimulation in both the presence and absence of extracellular Ca^{2+}. A different spatial distribution of IP_3 receptor isoforms in cardiomyocytes was found. Ryanodine did not prevent the IGF-1-induced increase of Ca^{2+}_i levels but inhibited the basal and spontaneous Ca^{2+}_i oscillations observed when cardiac myocytes were incubated in Ca^{2+}-containing resting media. Spatial analysis of fluorescence images of IGF-1-stimulated cardiomyocytes incubated in Ca^{2+}-containing resting media showed an early increase in Ca^{2+}_i, initially localized in the nucleus. Calcium imaging suggested that part of the Ca^{2+} released by stimulation with IGF-1 was initially contained in the perinuclear region. The IGF-1-induced increase on Ca^{2+}_i levels was prevented by 1,2-bis(2-aminophenoxy)ethane-*N*,*N*,*N*′,*N*′-tetraacetic acid-AM, thapsigargin, xestospongin C, 2-aminoethoxy diphenyl borate, U-73122, pertussis toxin, and βARKct (a peptide inhibitor of Gβγ signaling). Pertussis toxin also prevented the IGF-1-dependent IP_3 mass increase. Genistein treatment largely decreased the IGF-1-induced changes in both Ca^{2+}_i and IP_3. LY29402 (but not PD98059) also prevented the IGF-1-dependent Ca^{2+}_i increase. Both pertussis toxin and U73122 prevented the IGF-1-dependent induction of both ERKs and protein kinase B. We conclude that IGF-1 increases Ca^{2+}_i levels in cultured cardiac myocytes through a Gβγ subunit of a pertussis toxin-sensitive G protein-PI3K-phospholipase C signaling pathway that involves participation of IP_3.

Insulin-like growth factor-1 (IGF-1)[1] plays important roles in numerous physiological processes, ranging from normal growth and development during the early stages of embryogenesis to the regulation of specific functions in several tissues and organs in later stages of development (1). IGF-1 and its receptor (IGF-1R) are present in rat heart, consistent with IGF-1 regulating growth and hypertrophy in the developing heart in an autocrine or paracrine manner (2). IGF-1 induces cardiac hypertrophy *in vitro* and *in vivo* (3–5); protective and anti-apoptotic properties for this growth factor have also been demonstrated in different models of myocardial ischemia and infarction (6–9).

IGF-1R, which is closely related to the insulin receptor, is a protein-tyrosine kinase composed of two heterodimers linked by disulfide bonds (10). Following IGF-1 binding, IGF-1R becomes autophosphorylated on several tyrosine residues, allowing its interaction with phosphotyrosine binding or Src homology 2 (SH2) domain-containing proteins, thereby transducing signals to downstream effectors (11). Through these effectors, IGF-1 activates two main signaling cascades, the Ras-Raf-mitogen-activated protein kinase (MEK)-extracellular signal-regulated kinase (ERK) and the phosphatidylinositol 3-kinase (PI3K)/protein kinase B (PKB/Akt) pathways (12). Several recent studies have demonstrated that IGF-1R also activates heterotrimeric G proteins in some cell types. Luttrell *et al.* (13) first demonstrated in rat-1 fibroblasts that treatment with pertussis toxin (PTX) or transfection with a Gβγ scavenger (βARK-CT) blocked IGF-1-induced ERK activation (13). This study suggested the involvement of the Gβγ subunit of a PTX-sensitive G protein in the activation of ERK (13). Similar results have been obtained with human intestinal smooth muscle cells (14), 3T3-L1 mouse pre-adipose cells (15), and rat cerebellar granule neurons (16).

Conflicting observations on the roles of intracellular calcium (Ca^{2+}) and inositol 1,4,5-trisphosphate (IP_3) in IGF-1 signaling have been reported. In BALB/c 3T3 cells, IGF-1 stimulates Ca^{2+} influx via IGF-1R by activating a Ca^{2+}-permeable cation channel (17). The resulting Ca^{2+} influx produces oscillations in the concentration of free intracellular Ca^{2+} ($[Ca^{2+}]_i$) independently of phosphoinositide turnover (18). In contrast, in cultured bovine alveolar macrophages, nanomolar concentrations of

* This work was supported in part by Fondo Nacional de Ciencia y Tecnología (FONDECYT) Grants 1010246 (to S. L.), FONDAP 15010006 (to S. L. and E. J.) Beca Apoyo Tesis-2002 and Graduate Grant UCH PG 75/2001 (to L. C.). The costs of publication of this article were defrayed in part by the payment of page charges. This article must therefore be hereby marked "*advertisement*" in accordance with 18 U.S.C. Section 1734 solely to indicate this fact.

¶ Supported by fellowships from the Consejo Nacional de Investigaciones Científicas y Técnicas, Chile.

‡‡ To whom correspondence may be addressed: Instituto de Ciencias Biomédicas, Facultad de Medicina, Universidad de Chile, Independencia 1027, Santiago 6640750, Chile. Tel.: 562-678-6510; E-mail: ejaimovi@machi.med.uchile.cl.

§§ To whom correspondence may be addressed: Departamento de Bioquímica y Biología Molecular, Facultad de Ciencias Químicas y Farmacéuticas, Universidad de Chile, Olivos 1007, Santiago 6640750, Chile. Tel.: 562-678-2919; Fax: 562-737-8920; E-mail: slavander@uchile.cl.

[1] The abbreviations used are: IGF-1, insulin-like growth factor 1; PI3K, phosphatidylinositol 3-kinase; PLC, phospholipase C; IP_3, inositol 1,4,5-trisphosphate; PKB, protein kinase B; MEK, mitogen-activated protein kinase kinase; ERK, extracellular signal-regulated kinase; PTX, pertussis toxin; MES, 2-(*N*-morpholino)ethanesulfonic acid; Ad adenovirus; $[Ca^{2+}]_i$, intracellular $[Ca^{2+}]$; TBST, Tris-buffered saline with Tween 20; ROI, region of interest; BAPTA, 1,2-bis(2-aminophenoxy)ethane-*N*,*N*,*N*′,*N*′-tetraacetic acid.

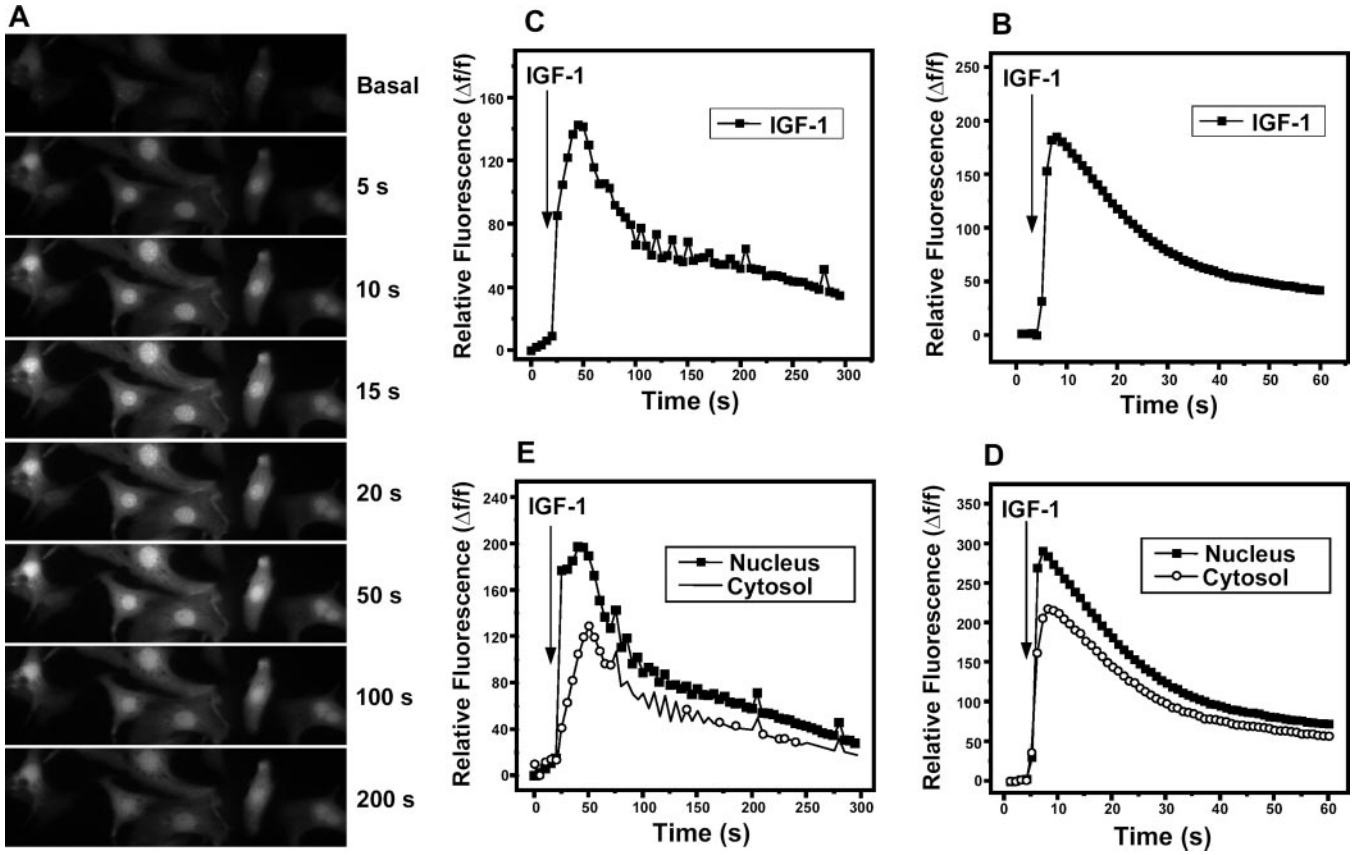

FIG. 1. **IGF-1 induces the intracellular Ca^{2+} level increase in the nucleus and cytosol of cultured rat cardiomyocytes.** Cells, maintained in Ca^{2+}-free resting media, were preloaded with Fluo3-AM and then stimulated with IGF-1 (1 nM). Using a fluorescence microscopy equipped with a CDD camera, serial Ca^{2+} images of Fluo3 fluorescence in a single cardiomyocyte were registered (*A*), relative total fluorescence (ratio of fluorescence difference, stimulated − basal ($F_i - F_o$), to basal value (F_o)) as a function of time of each image were calculated (*B*). Relative total fluorescence of Fluo3-AM-preloaded cardiomyocytes incubated in Ca^{2+}-containing resting media and stimulated with IGF-1 (1 nM) (*C*) and ROI analysis of fluorescence images of a cardiomyocyte nucleus and cytosol maintained in Ca^{2+} free (*D*) and Ca^{2+} containing resting media (*E*) were measured.

IGF-1 stimulate after 30 s the accumulation of IP_3 and inositol 1,3,4,5-tetraphosphate, and induce a rise in $[Ca^{2+}]_i$ (19). In chondrocytes, IGF-1 induces Ca^{2+} release from the endoplasmic reticulum, which is partially blocked by phospholipase C (PLC) inhibitors and PTX (20). Short term exposure of neurons and neuronal cell lines to IGF-1 leads to direct activation of voltage-gated L-type Ca^{2+} channels (21–23), whereas in rat pinealocytes IGF-1 inhibits L-type currents (24). IGF-1 also modulates L-type Ca^{2+} channels in adult rat cardiac myocytes and in skeletal muscle of young and middle-aged rats, but not of aged rats (25, 26). In whole heart and in ferret papillary muscle, IGF-1 displays an acute positive inotropic effect, which is secondary to augmented myofilament responsiveness to Ca^{2+} (27). In rat ventricular papillary muscle cells, however, acute exposure to IGF-1 or insulin results in enhanced muscle contractility that is associated with $[Ca^{2+}]_i$ transients (28).

In cardiac myocytes, IGF-1 activates multiple signaling pathways, including ERK-PKC, PKB/PI3K, PLC-γ, and JAK-STAT (9, 29, 30, 32). However, the role of cytosolic Ca^{2+} as the second messenger in the complex IGF-1 signaling pathways present in cardiac myocytes has not been examined.

In the present study we show that, both in the presence or absence of extracellular Ca^{2+}, addition of IGF-1 to cultured cardiac myocytes induced a rapid $[Ca^{2+}]$ increase in both the nucleus and cytoplasm and also produced a rapid increase of IP_3 levels. The presence of extracellular Ca^{2+} modified the kinetics of the $[Ca^{2+}]$ increase, delaying an increase of cytosolic but not nuclear $[Ca^{2+}]$. The role of tyrosine kinase, G-protein, PI3K, PLC, and the IP_3 receptor in the pathway leading to these calcium signals was established using specific inhibitors.

EXPERIMENTAL PROCEDURES

Materials—[^{3}H]IP_3 was from PerkinElmer Life Sciences. Fluo3-acetoxymethyl ester (Fluo3-AM) was from Molecular Probes (Eugene, OR). Thapsigargin, xestospongin C, genistein, BAPTA-acetoxymethyl ester (BAPTA-AM), LY294002 (LY), PD98059 (PD), and SB203580 (SB) were from Calbiochem-Novabiochem Corp. (San Diego, CA). 2-Aminoethoxy diphenyl borate was from Aldrich. Polyclonal antibodies against type 1 and type 2 IP_3 receptor were from Affinity BioReagents (Golden, CO) and Santa Cruz Biotechnology (Santa Cruz, CA), respectively. Anti-type 3 IP_3 receptor was kindly donated by G. A. Mignery (Loyola University, Chicago, IL). Polyclonal antibodies against phosphorylated (Ser^{473}) PKB, total PKB, phosphorylated (Thr^{202}/Thr^{204}) ERK, and total ERK were from Cell Signaling Technology Inc. (Beverly, MA). Dulbecco's modified Eagle's medium, medium 199, U-73122, ryanodine, nifedipine, PTX, IP_3, and other biochemicals were purchased from Sigma unless stated otherwise. Human recombinant IGF-1 was donated by Dr. C. George-Nascimento (Austral Biologicals, San Ramon, CA).

Animals—Rats were bred in the Animal Breeding Facility from the Faculty of Chemical and Pharmaceutical Sciences, University of Chile (Santiago, Chile). We performed all studies with the approval of the institutional bioethical committee at the Faculty of Chemical and Pharmaceutical Sciences, University of Chile, Santiago. This investigation conforms to the "Guide for the Care and Use of Laboratory Animals" published by the United States National Institutes of Health (31).

Culture of Cardiac Myocytes—Cardiac myocytes were prepared from hearts of 1–3-day-old Sprague-Dawley rats as described previously (29). For IP_3 determination, cardiomyocytes were plated at a final density of 0.7×10^3/mm^2 on gelatin-precoated 60-mm dishes. For detection of Ca^{2+}, cells were plated with a final density of 1.0×10^3/mm^2 on gelatin-precoated coverslips. Serum was withdrawn for 24 h before the

cells were treated further with agonist IGF-1 (1–100 nM) in serum-free medium (Dulbecco's modified Eagle's medium/medium 199) at 37 °C. Cultured cardiomyocytes, assessed with an anti-β-myosin heavy chain antibody, were at least 95% pure.

Recombinant Adenoviruses—Adenoviral vectors (Ad) were propagated and purified as previously described (33). Two transgenes (a gift from Dr. W. J. Koch, Duke University Medical Center, Durham, NC) were used: βARKct (Ad-βARKct) and an empty viral construct (Ad-EV). βARKct is a peptide inhibitor of Gβγ signaling (34). Cardiomyocytes were infected with adenoviral vectors at a multiplicity of infection of 300.

Determination of IP_3 Mass—Cardiomyocytes were rinsed and preincubated for 20 min at room temperature in 58 mM NaCl, 4.7 mM KCl, 3 mM $CaCl_2$, 1.2 mM $MgSO_4$, 0.5 mM EDTA, 60 mM LiCl, 10 mM glucose, and 20 mM Hepes, pH 7.4. Cells were stimulated by fast (1 s) replacement of this solution by a solution containing IGF-1. At the times indicated, the reaction was stopped by rapid aspiration of the stimulating solution, addition of 0.8 M ice-cold perchloric acid and freezing with liquid nitrogen. Samples were allowed to thaw and cell debris was spun down for protein determination. The supernatant was neutralized with a solution of 2 M KOH, 0.1 M MES, and 15 mM EDTA. The neutralized extracts were frozen at −80 °C until required for IP_3 determination. Measurements of IP_3 mass were made by radioreceptor assay (35). Briefly, a crude rat cerebellum membrane preparation was obtained after homogenization of tissue in 50 mM Tris-HCl, pH 7.7, containing 1 mM EDTA, 2 mM β-mercaptoethanol and centrifugation at 20,000 × *g* for 15 min. This procedure was repeated 3 times, suspending the final pellet in the same solution plus 0.3 M sucrose and freezing it at −80 °C until required for use. The rat cerebellar membrane preparation was calibrated for IP_3 binding with 1.6 nM [^{3}H]IP_3 and 2–120 nM cold IP_3, with sample analysis performed in a similar way but replacing cold IP_3 with a portion of the neutralized supernatant. [^{3}H]IP_3 radioactivity, which remained bound to membranes, was measured in a Beckman LS-6000TA liquid scintillation spectrometer (Beckman Instruments Corp., Fullerton, CA). Protein was determined by the Lowry method (36).

Measurement of Intracellular Calcium—Cellular calcium images were obtained from neonatal cardiac myocytes preloaded with Fluo3-AM, using an inverted confocal microscope (Carl Zeiss Axiovert 135 M-LSM Microsystems) or a fluorescence microscope (Olympus Diaphot-TMD, Nikon Corporation) equipped with a cooled CCD camera and image acquisition system (Spectra Source MCD 600). Cardiac myocytes were washed three times with Ca^{2+}-containing resting media (Krebs buffer: 145 mM NaCl, 5 mM KCl, 2.6 mM $CaCl_2$, 1 mM $MgCl_2$, 10 mM HEPES-Na, 5.6 mM glucose, pH 7.4) to remove Dulbecco's modified Eagle's medium/medium 199 culture medium, and loaded with 5.4 μM Fluo3-AM (coming from a stock in 20% pluronic acid, Me_2SO) for 30 min at room temperature. After loading, cardiac myocytes were washed either with the same buffer or with a Ca^{2+}-free resting media (145 mM NaCl, 5 mM KCl, 1.0 mM EGTA, 1 mM $MgCl_2$, 10 mM HEPES-Na, 5.6 mM glucose, pH 7.4) and used within 2 h. The cell-containing coverslips were mounted in a 1-ml capacity plastic chamber and placed in the microscope for fluorescence measurements after excitation with a 488-nm wavelength argon laser beam or filter system. IGF-1 was either added directly or the solution was fast (1 s) changed in the chamber. The fluorescent images were collected every 0.4–2.0 s for fast signals and analyzed frame by frame with the image data acquisition program (Spectra-Source) of the equipment. An objective lens PlanApo 60X (numerical aperture 1.4) was generally used. In most of the acquisitions, the image dimension was 512 × 120 pixels. Intracellular calcium was expressed as a percentage of fluorescence intensity relative to basal fluorescence (a value stable for at least 5 min in resting conditions). The fluorescence intensity increase is proportional to the rise in $[Ca^{2+}]_i$ (37).

Digital Image Processing—Elimination of out-of-focus fluorescence was performed using both the "no neighbors" deconvolution algorithm and Castleman's (38) point spread function theoretical model, as described previously (39). For quantitation of fluorescence, the summed pixel intensity was calculated from the section delimited by a contour. As a way of increasing efficiency of these data manipulations, action sequences were generated. To avoid interference in the fluorescence by possible IGF-1 effects on the cellular volume, the area of each fluorescent cell was determined by image analysis using adaptive contour and then creating a binary mask, which was compared with its bright-field image.

Western Blot Analysis—Cell lysates were matched for proteins (10–40 μg) and were separated by SDS-PAGE on 10% polyacrylamide gels and electrotransferred to nitrocellulose. Membranes were blocked with 5% nonfat milk powder in Tris-buffered saline (TBS) (pH 7.6)

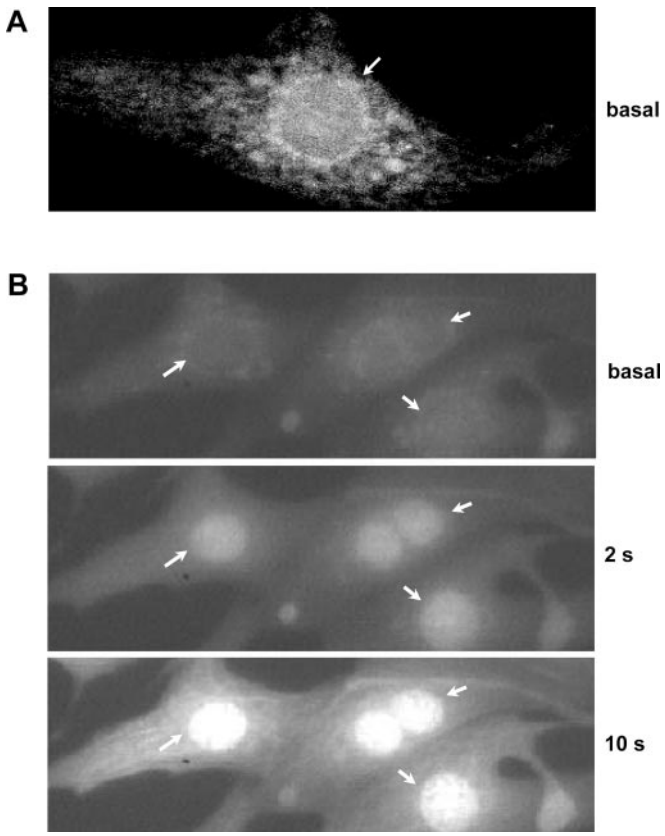

FIG. 2. **IGF-1 induces Ca^{2+} release from perinuclear stores in cardiomyocytes.** *A*, reconstitution of a multislice imaging of a Fluo3-AM-preloaded basal cardiomyocyte, obtained by confocal microscopy. Cardiomyocyte was maintained in Ca^{2+}-free resting media. *B*, serial Ca^{2+} images of Fluo3-AM-preloaded cardiomyocytes, maintained in Ca^{2+}-free resting media and stimulated with IGF-1 (10 nM), were obtained by epifluorescence microscopy. *Arrows* indicate perinuclear basal fluorescence.

containing 0.1% (v/v) Tween 20 (TBST) for 60 min at room temperature. Primary antibodies were diluted 1/1,000 in blocking solution. Nitrocellulose membranes were incubated with primary antibodies overnight at 4 °C. After washing in TBST (3× 10 min each), the blots were incubated for 2 h at room temperature with horseradish peroxidase-linked secondary antibody (1:5,000 in 1% (w/v) nonfat milk powder in TBST). The blots were washed again in TBST and the bands were detected using ECL with exposure to Kodak film for 0.5–30 min. Blots were quantified by scanning densitometry.

Subcellular Fractionation—Nuclear and cytosolic fractions from cultured cardiac myocytes were prepared as described by Schreiber *et al.* (40). Homogeneity of fractions were assessed by Western blot using α-actinin (marker for myofibril Z bands) (41), lamina-associated polypeptide 2 (marker for nuclear inner membrane) (42), and calsequestrin (marker for sarcoplasmic reticulum) (43).

Immunocytochemistry—Cardiomyocytes grown on coverslips were fixed in iced methanol, blocked in phosphate-buffered saline containing 1% bovine serum albumin for 30 min, and incubated with primary anti-IP_3 receptor antibodies at 4 °C overnight. The cells were then washed 5-fold with phosphate-buffered saline/bovine serum albumin and incubated with the appropriate goat anti-rabbit secondary antibody for 1 h at room temperature. After washing three more times, the coverslips were mounted in Vectashield (Vector Laboratories, Inc.). The samples were evaluated in a scanning confocal microscope (Carl Zeiss Axiovert 135, LSM Microsystems) and documented through computerized images (44).

Expression of Results and Statistical Analysis—Data are represented as mean ± S.E. of the number of independent experiments indicated (*n*) or as examples of representative experiments performed on at least three separate occasions. Data were analyzed by analysis of variance and comparisons between groups were performed using a protected Tukey's *t* test. A value of $p < 0.05$ was set as the limit of statistical significance.

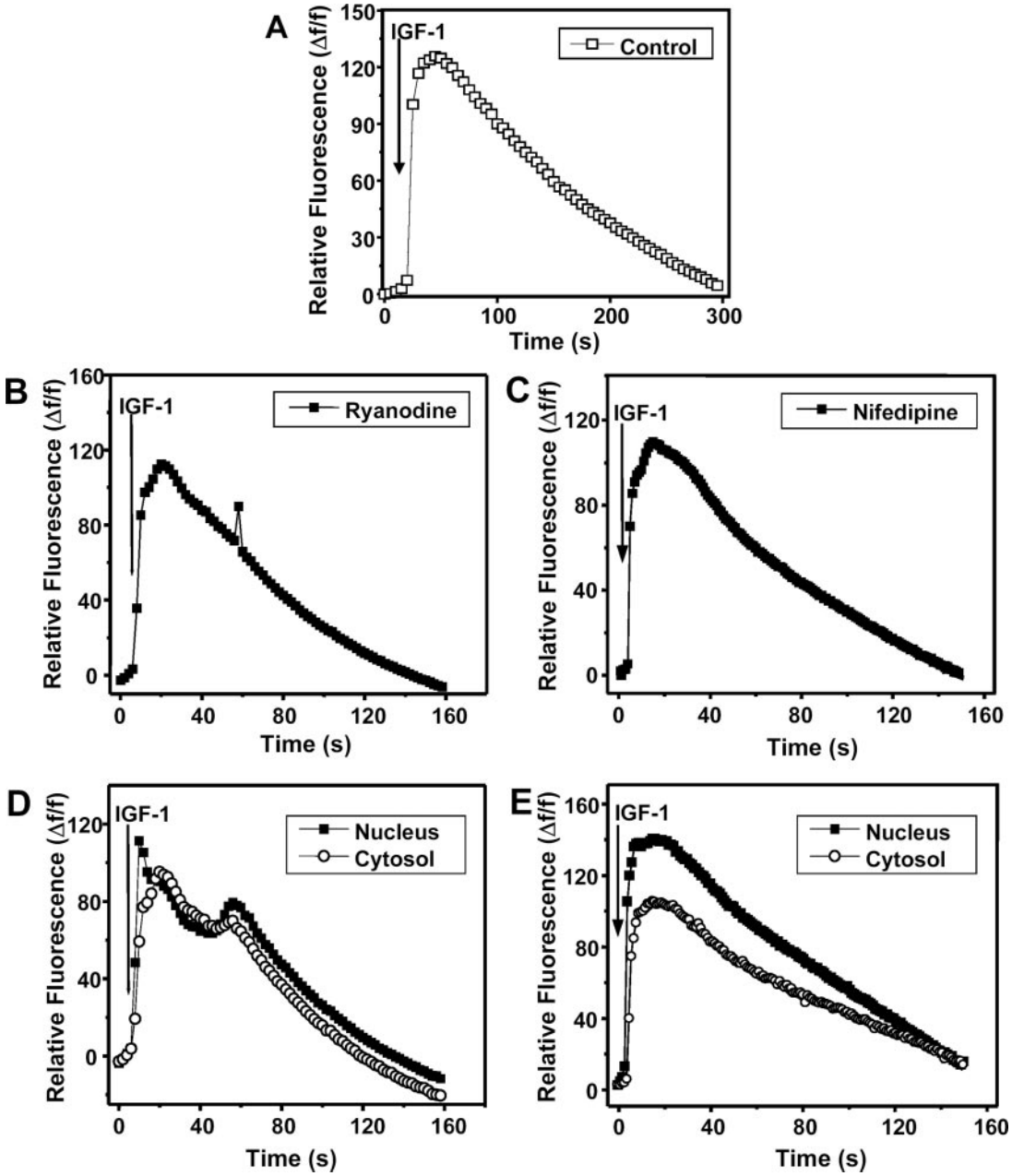

FIG. 3. **Effect of ryanodine and nifedipine in the IGF-1-induced Ca^{2+} transients in cultured rat cardiomyocytes.** Fluo3-AM-preloaded cardiomyocytes, maintained in Ca^{2+}-free resting media, were preincubated with (*A*) culture media as control (*B*) ryanodine (20 μM) or (*C*) nifedipine (10 μM) for 30 min and then stimulated with IGF-1 (1 nM). Fluo3 fluorescence images were registered and relative fluorescence was calculated. ROI analysis of fluorescence images of a IGF-1-stimulated cardiomyocyte nucleus and cytosol preincubated with (*D*) ryanodine or (*E*) nifedipine were obtained.

RESULTS

IGF-1-induced Intracellular Ca^{2+} Transients in Rat Cardiac Myocytes—Changes in intracellular Ca^{2+} concentration, $[Ca^{2+}]_i$, were visualized in single cardiomyocytes preloaded with Fluo3-AM. Increases of relative fluorescence represent an increase of free cytosolic $[Ca^{2+}]$. Multiple region of interest (ROI) analysis of single cells revealed that similar kinetics and fluorescence intensities were detected disregarding the analyzed ROI window (data not shown). Quiescent cardiomyocytes, maintained in Ca^{2+}-containing resting solution, exhibited basal $[Ca^{2+}]_i$ oscillations that were blocked by 30 min preincubation with ryanodine (50 μM) (data not shown). Incubation of cardiomyocytes in resting solution without Ca^{2+} also prevented $[Ca^{2+}]_i$ oscillations (data not shown).

Addition of IGF-1 (1 nM) to cardiomyocytes maintained in Ca^{2+}-free resting solution induced a fast and transient (10–20 s) increase in $[Ca^{2+}]_i$, with a maximum at 4–5 s after IGF-1 addition (Fig. 1, *A* and *B*). The lowest concentration of IGF-1 that induced $[Ca^{2+}]_i$ transients was 0.01 nM. When cardiomyocytes were maintained in Ca^{2+}-containing resting solution, addition of IGF-1 induced a similar, although slower increase of $[Ca^{2+}]_i$, reaching a maximum 40–50 s after IGF-1 addition (Fig. 1*C*). Cardiomyocytes maintained in Ca^{2+}-containing resting solution usually showed basal $[Ca^{2+}]_i$ oscillations; these oscillations were not altered by addition of IGF-1. Following IGF-1 addition in Ca^{2+}-free resting solution, an increase of $[Ca^{2+}]_i$ was observed both in the nucleus and cytoplasm (Fig. 1*A*). Analysis of ROI in the fluorescence images showed that both nuclear and cytosolic Ca^{2+} transient time courses were similar in IGF-1-stimulated cardiomyocytes maintained in the

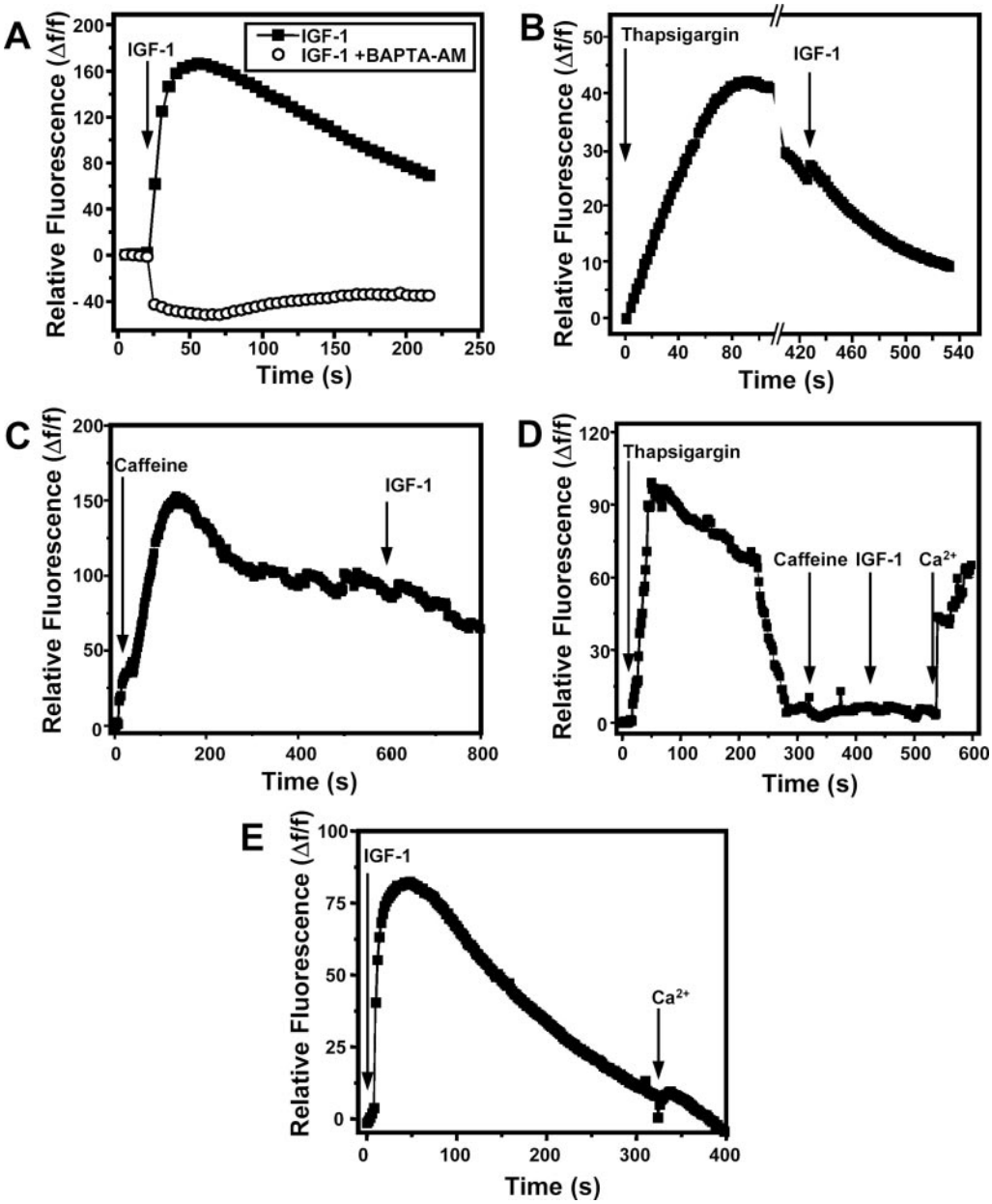

FIG. 4. **Effect of BAPTA-AM and thapsigargin on the IGF-1-induced Ca^{2+} transients in cultured rat cardiomyocytes.** Fluo3-AM-preloaded cardiomyocytes, maintained in Ca^{2+}-free resting media, were preincubated with: *A*, BAPTA-AM (100 μM) for 30 min and then stimulated with IGF-1 (1 nM); *B*, thapsigargin (1 μM) and 5 min later stimulated with IGF-1 (1 nM); *C*, caffeine (5 mM) and 7.5 min later stimulated with IGF-1 (1 nM); *D*, thapsigargin (500 μM) and 6 min later treated with caffeine (5 mM) and 3 min later treated with Ca^{2+} (2 mM); or *E*, IGF-1 (1 nM) and 6.25 min later treated with Ca^{2+} (2 mM). Fluo3 fluorescence images were registered and relative fluorescence was calculated.

Ca^{2+}-free resting solution (Fig. 1*D*). However, when cardiomyocytes were treated with IGF-1 in Ca^{2+}-containing resting solution, nuclear $[Ca^{2+}]$ increased faster than cytosolic $[Ca^{2+}]$ (Fig. 1*E*). ROI analysis clearly showed that extracellular Ca^{2+} slowed down the cytosolic but not the nuclear increase in $[Ca^{2+}]$ stimulated by IGF-1 (Fig. 1, *D* and *E*). Rates of rise of the nuclear Ca^{2+} transients in the presence and absence of external Ca^{2+} were 32.3 ± 7.6 and 38.6 ± 8.1 ($\Delta f/f$ per s) (n = 4), respectively. However, rates of rise of Ca^{2+} transients in the cytosol were 3.9 ± 1.4 and 20.1 ± 5.3 ($\Delta f/f$ per s) (n = 10), respectively. In all cells studied, the IGF-1-induced increase in $[Ca^{2+}]$ did not trigger regenerative waves through the cytosol.

IGF-1-induced Ca^{2+} Release from Ryanodine and Nifedipine-insensitive Intracellular Stores—The increase in $[Ca^{2+}]_i$ in cardiomyocytes upon stimulation with IGF-1 in the absence of extracellular Ca^{2+} suggests involvement of Ca^{2+} release from internal stores. Resting Fluo3-AM preloaded cardiomyocytes usually displayed increased basal fluorescence in the perinuclear region (Fig. 2, *A* and *B*). After addition of IGF-1, the distribution of fluorescence changed and the increase in fluorescence was homogeneous in both the nucleus and cytoplasm (Fig. 2*B*, *2 s* and *10 s*). These observations suggest that IGF-1 induced Ca^{2+} release from perinuclear Ca^{2+} stores.

IGF-1-induced Ca^{2+} transients in cardiomyocytes maintained in Ca^{2+}-free resting media were not suppressed by ryanodine (Fig. 3*B*). However, ROI analysis of nuclear and cytosolic fluorescence revealed that in the presence of ryanodine the increase in cytosolic $[Ca^{2+}]$ was slower than in the nucleus (Fig. 3*D*). Cardiomyocytes incubated in Ca^{2+}-containing resting solution displayed an analogous behavior. These results suggest that the IGF-1 stimulated fast increase in cytoplasmic Ca^{2+} was partly because of calcium release through ryanodine receptors because a fast component was inhibited after preincubation with 20 μM ryanodine.

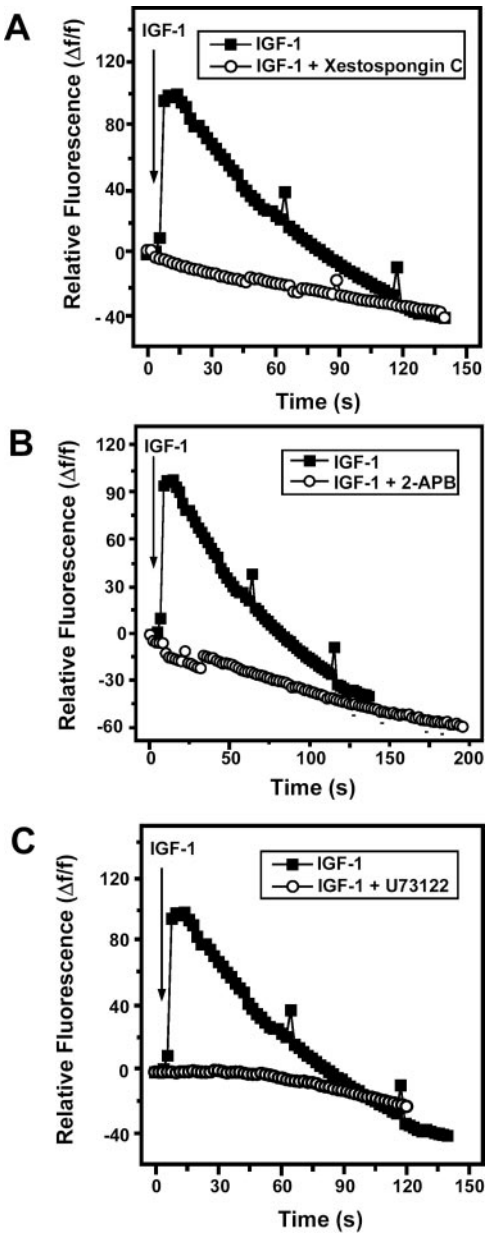

FIG. 5. **Effect of IP_3-mediated Ca^{2+} release and phospholipase C inhibitors on the Ca^{2+} transients induced by IGF-1.** Fluo3-AM-preloaded cardiomyocytes, maintained in Ca^{2+}-free resting media, were preincubated with: *A*, xestospongine C (100 μM); *B*, 2-aminoethoxy diphenyl borate (20 μM); and *C*, U-73122 (50 μM) for 30 min, and then stimulated with IGF-1 (1 nM). Fluo3 fluorescence images were registered and relative fluorescence was calculated.

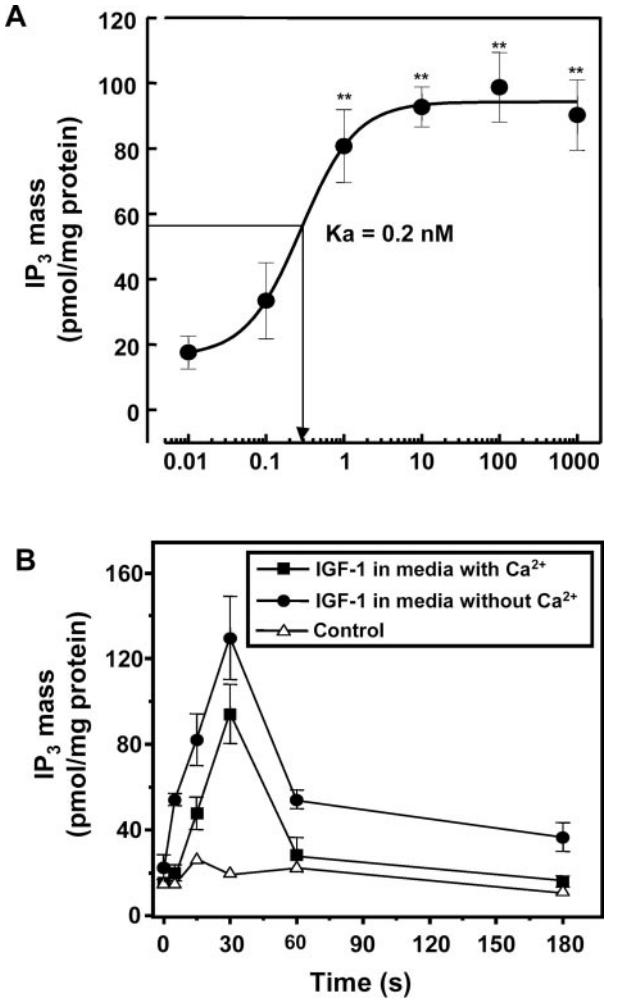

FIG. 6. **Effect of IGF-1 on IP_3 mass in cultured rat cardiomyocytes.** *A*, cardiomyocytes were treated with different concentrations of IGF-1 (0.01–1,000 nM) for 30 s and cell-free extracts were prepared. *B*, cardiomyocytes were treated with IGF-1 (1 nM) and at different times (0–180 s) cell-free extracts were prepared. IP_3 mass was determined in cell-free extracts as described under "Experimental Procedures." Values represent the average of three different experiments ± S.D. **, $p < 0.01$ and *, $p < 0.05$ *versus* time 0 min.

Nifedipine did not modify IGF-1-induced Ca^{2+} transients in cardiomyocytes maintained in Ca^{2+}-free resting solution (Fig. 3*C*). ROI analysis of images revealed that both nuclear and cytosolic fluorescence increases presented similar kinetics in the presence or absence of nifedipine (Fig. 3*C*). These results suggest that voltage-dependent L-type Ca^{2+} channels are not involved in the IGF-1-induced Ca^{2+} transients in cardiomyocytes.

To further demonstrate the role of intracellular Ca^{2+} stores in the generation of IGF-1-induced Ca^{2+} transients, cardiomyocytes were preloaded with both BAPTA-AM and Fluo3-AM, and then stimulated with 1 nM IGF-1. BAPTA-AM inhibited the increase of fluorescence induced by IGF-1 and only a small decrease in fluorescence was apparent in these conditions (Fig. 4*A*). Treatment of Fluo3-AM-preloaded cardiomyocytes with thapsigargin, a sarco/endoplasmic reticulum Ca^{2+}-ATPase inhibitor, led to a slow increase of intracellular fluorescence because of Ca^{2+} loss from internal stores. Subsequent addition of IGF-1 (5 min) to these cells did not induce the characteristic increase in the fluorescence signal (Fig. 4*B*). Similar results were obtained when internal Ca^{2+} stores where depleted using caffeine, a ryanodine receptor activator (Fig. 4*C*).

When thapsigargin-pretreated cardiomyocytes were incubated with caffeine, no additional Ca^{2+} release was detected (Fig. 4*D*). Further treatment with IGF-1 did not increase fluorescence, an effect obtained by the addition of external Ca^{2+} (Fig. 4*D*). This Ca^{2+} influx elicited by calcium add back suggests the activation of a plasma membrane store-operated channel activity in neonatal rat cardiac myocytes. However, external Ca^{2+} addition to cardiac myocytes after IGF-1 treatment showed a low increase of $[Ca^{2+}]_i$, indicating that IGF-1 poorly induced the capacitative calcium entry (Fig. 4*E*). These results indicate that in cardiomyocytes Ca^{2+} is released from internal stores, sensitive to both caffeine and thapsigargin, probably located at the perinuclear region, after IGF-1 stimulation.

IGF-1 Induction of Ca^{2+} Transients Was Dependent on IP_3 Receptors and IP_3 Production—Xestospongin C and 2-aminoethoxy diphenyl borate, inhibitors of IP_3-mediated Ca^{2+} re-

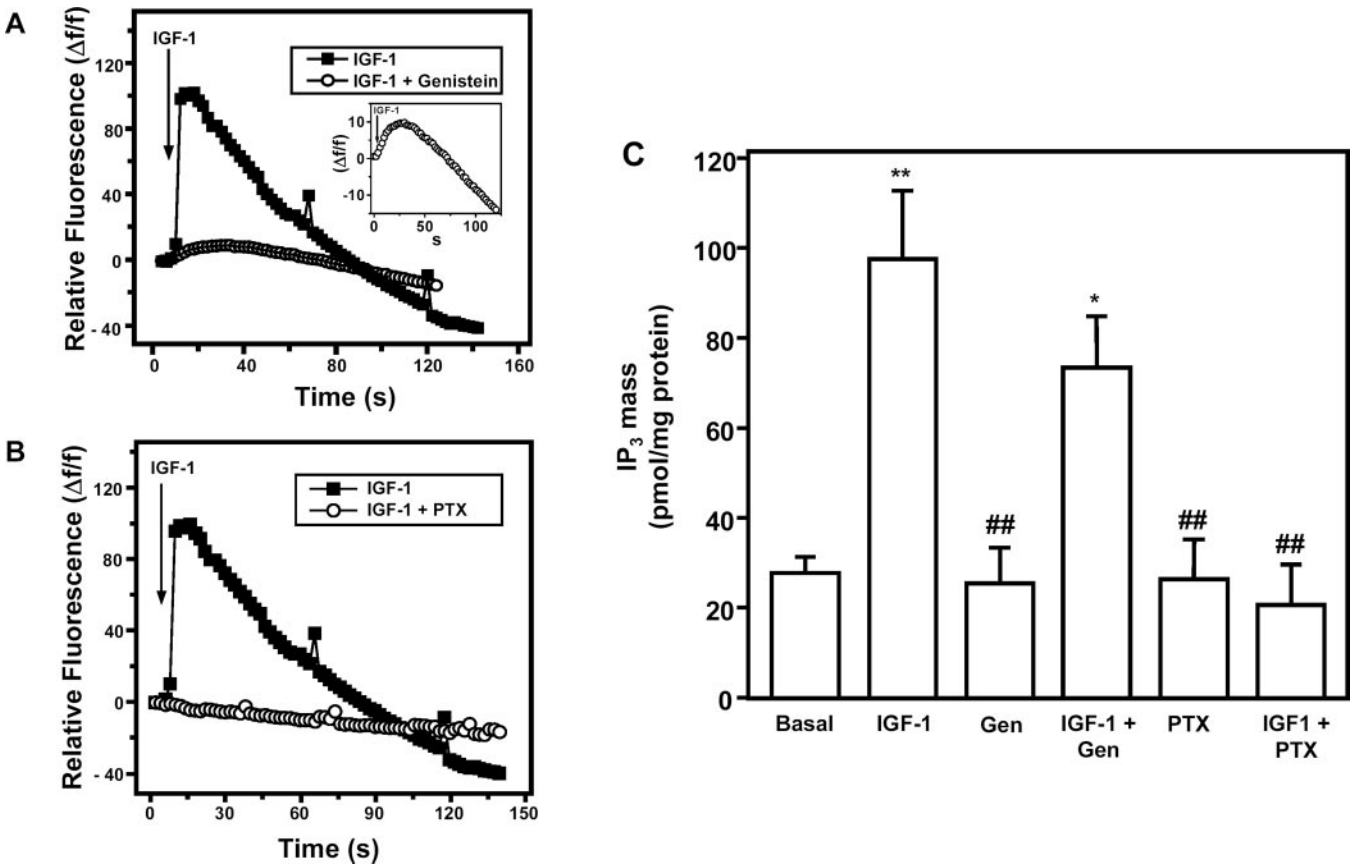

FIG. 7. **Effect of PTX and genistein on the IGF-1-induced Ca^{2+} transient and IGF-1-induced IP_3 mass increase in rat cardiomyocytes.** Fluo3-AM-preloaded cardiomyocytes, maintained in Ca^{2+}-free resting media, were preincubated with (*A*) genistein (100 μM) for 30 min, and (*B*) PTX (1 μg/ml) for 60 min, and then stimulated with IGF-1 (1 nM). Fluo3 fluorescence images were registered and relative fluorescence was calculated. *Inset graph* in *panel A* represents a re-scaled curve of Ca^{2+} response to IGF-1 in the presence of genistein (100 μM). *C*, cardiomyocytes were treated with PTX (1 μg/ml) for 60 min or genistein (*Gen*, 100 μM) for 30 min, and then stimulated with IGF-1 (1 nM). After 30 s cell-free extracts were prepared and IP_3 mass was determined as described under "Experimental Procedures." Values represent the average of three different experiments ± S.D. **, $p < 0.01$; *, $p < 0.05$ *versus* basal; ##, $p < 0.01$ *versus* IGF-1.

lease, inhibited IGF-1-induced Ca^{2+} transients in cardiomyocytes (Fig. 5, *A* and *B*). Furthermore, U-73122, an inhibitor of agonist-induced PLC activation, blocked the increase in $[Ca^{2+}]_i$ induced by IGF-1 (Fig. 5*C*). These results suggest that IGF-1-induced Ca^{2+} release from internal stores is a PLC-mediated/IP_3-dependent process.

Furthermore, IGF-1 induced a significant IP_3 mass increase in cardiomyocytes. A dose-response study determined that concentrations of IGF-1 ≥ 1 nM induced a maximal increase of IP_3 mass, with K_a = 0.3 nM (Fig. 6*A*). In cardiomyocytes incubated in a Ca^{2+}-free resting solution, a time course analysis showed that IGF-1 induced a significant IP_3 mass increase at 5 s, with a maximum at 30 s post-stimulus (Fig. 6*B*). However, when cardiomyocytes were incubated in Ca^{2+}-containing resting solution, IGF-1 induced a significant IP_3 mass increase only after 15 s, reaching maximal levels 30 s poststimulus (Fig. 6*B*). The basal mass of IP_3 was ~20 pmol/mg of protein; IGF-1 stimulation increased this value to 90 and 130 pmol/mg of protein (4.5- and 6.5-fold increase) for cardiomyocytes incubated in Ca^{2+}-free and Ca^{2+}-containing resting media, respectively (Fig. 6*B*). These results indicate that IGF-1-induced Ca^{2+} transient kinetics was associated with an IP_3 mass increase.

Effect of Pertussis Toxin and Genistein on the IGF-1-induced Ca^{2+} Transients and IP_3 Mass Increase—Several reports indicate that IGF-1 activates different intracellular signaling cascades through both protein-tyrosine kinase and G_i protein mechanisms (13–16). To assess both possibilities, Fluo3-AM-preloaded cardiomyocytes in Ca^{2+}-free resting media were preincubated for 45 min with genistein or PTX and then stimulated with IGF-1. As shown in Fig. 7, *A* and *B*, IGF-1-induced Ca^{2+} transients were largely inhibited by genistein, whereas PTX totally blocked these signals. Preincubation of cardiomyocytes with PTX also completely inhibited the IP_3 mass increase induced by IGF-1, whereas genistein exerted only a partial inhibitory effect (Fig. 7*C*). These results suggest that the signaling cascade induced via the IGF-1 receptor requires the combined participation of both protein-tyrosine kinase and PTX-sensitive G protein to induce Ca^{2+} transients and to increase the mass of IP_3.

Effect of a Peptide Inhibitor of Gβγ Signaling on the IGF-1-induced Ca^{2+} Transients—To further determine which subunits of trimeric G_i proteins are essential to the IGF-1-induced Ca^{2+} transients, myocytes were infected by Ad-βARKct (34, 45). Similar to PTX treatment, βARKct effectively abolished the IGF-1-induced Ca^{2+} transients (Fig. 8). This result indicates that Gβγ subunits dissociated from G_i proteins are critical components of the IGF-1-induced Ca^{2+} transients in cardiac myocytes.

PI3K but Not MEK1 Is Involved in the IGF-1-dependent Ca^{2+} Transients—The two major routes for IGF-1 receptor signaling are the PI3K and the ERK pathways (21–23). To determine whether IGF-1-induced Ca^{2+} transients involve previous activation of PI3K or MEK/ERK signaling pathways, we used chemical inhibitors of PI3K (LY294002 or LY) and MEK1 (PD98059 or PD). Fluo3-AM-preloaded cardiomyocytes incubated in Ca^{2+}-free resting media were preincubated with ei-

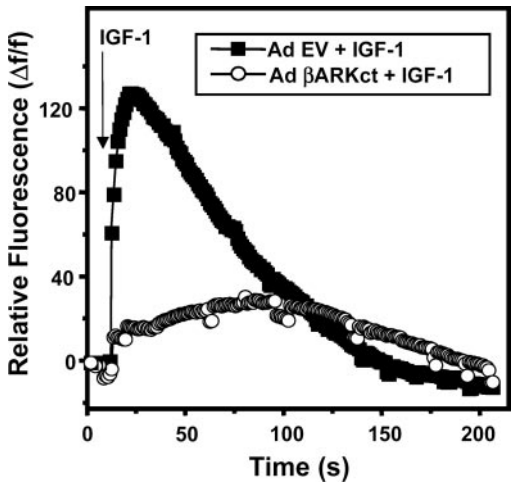

FIG. 8. **Effect of a peptide inhibitor of Gβγ signaling on the IGF-1-induced Ca^{2+} transients in rat cardiomyocytes.** Cardiomyocytes were transfected with either an adenovirus encoding a peptide derived from βARK1 (*Ad-βARKct*) or an empty virus (*Ad-EV*) as control. After 48 h, cardiomyocytes were preloaded with Fluo3-AM and maintained in Ca^{2+}-free resting media. Cells were then stimulated with IGF-1 (1 nM). Fluo3 fluorescence images were registered and relative fluorescence was calculated.

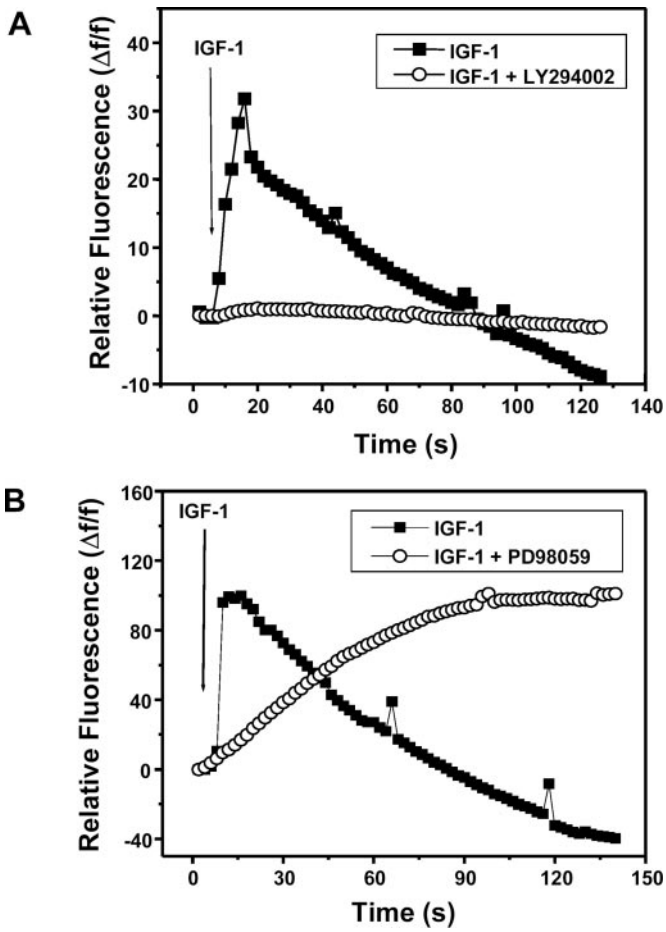

FIG. 9. **Participation of ERK and PI3K signaling pathways in the IGF-1-induced Ca^{2+} transients.** Fluo3-AM-preloaded cultured rat cardiomyocytes, maintained in Ca^{2+}-free resting media, were preincubated with (*A*) LY294002 (50 μM) or (*B*) PD98059 (100 μM) for 30 min, and then stimulated with IGF-1 (1 nM). Fluo3 fluorescence images were registered and relative fluorescence was calculated.

ther LY or PD and then treated with IGF-1. LY completely suppressed IGF-1-induced Ca^{2+} transients, but PD only slowed down the kinetics of the response (Fig. 9, *A* and *B*). These results suggest that while PI3K participates directly in the IGF-1-induced Ca^{2+} transient, the MEK/ERK pathway only modulates this signal.

To evaluate whether IGF-1 activation of ERK and PI3K pathways requires previous Ca^{2+} release, cultured cardiomyocytes were pretreated with PTX, BAPTA-AM, or U-73122, and then stimulated with IGF-1. PTX blocked IGF-1-stimulated phosphorylation of ERK1/2 but not of PKB (Fig. 10, *A* and *B*). These results are consistent with previous reports indicating that IGF-1-dependent ERK activation requires both tyrosine kinase activity and PTX-sensitive G protein, while the PI3K/PKB signaling pathway requires only tyrosine kinase activity (13–16). U-73122 but not BAPTA-AM inhibited IGF-1-dependent activation of both ERK1 and ERK2 (Fig. 10, *A* and *B*). BAPTA-AM and U-73122 did not modify IGF-1-dependent activation of PKB (Fig. 10*B*). Together, these results indicate that IGF-1-dependent activation of ERK but not of PKB required previous Ca^{2+} release.

IP_3 Receptor Isoforms Are Located Differentially within Cardiac Myocytes—To explain the specificity and compartmentalization of the IGF-1-induced Ca^{2+} transients, the presence of different IP_3 receptor isoforms was investigated in cardiomyocytes by immunoblotting. Cardiomyocytes expressed type 1, type 2, and type 3 IP_3 receptor isoforms (Fig. 11). Western blots of nuclear and cytosolic fractions revealed that type 1 and type 3 IP_3 receptors were mainly located in the nuclear fraction, whereas type 2 IP_3 receptor was located almost exclusively in the cytosolic fraction (Fig. 11).

The intracellular localization of IP_3 receptor isoforms was monitored by immunofluorescence labeling and confocal microscopy. As shown in Fig. 11, fluorescence because of the type 1 IP_3 receptor was seen primarily in the nuclear envelope and some cytosolic structures. The staining of type 1 IP_3 receptor appears to be continuous around the nuclear envelope. On the other hand, immunoreactivity against type 2 IP_3 receptor was located almost exclusively in cytoplasmic structures, with no presence in the nucleus (Fig. 11). Finally, the antibody against type 3 IP_3 receptor shows a significant amount of internal nuclear labeling as a punctuate pattern. This fluorescence pattern was also observed throughout the cellular matrix. These results indicate that there is a different spatial distribution of IP_3 receptor isoforms in cardiomyocytes.

DISCUSSION

Summary of Main Findings—In the present study, we show for the first time that IGF-1 induced a fast and transient increase in $[Ca^{2+}]_i$ in cultured rat cardiomyocytes. This Ca^{2+} was released from intracellular stores through an IP_3-dependent mechanism, essentially independent of ryanodine receptors or extracellular Ca^{2+} entry. Our results also indicate that the effect of IGF-1 on calcium increase was dependent on both tyrosine kinase activity and βγ subunits of a PTX-sensitive G protein.

IGF-1 Increased $[Ca^{2+}]_i$ in Cultured Cardiac Myocytes through an IP_3-dependent Mechanism—We described an IGF-1-dependent $[Ca^{2+}]_i$ increase in cultured rat cardiomyocytes; this $[Ca^{2+}]_i$ increase was not because of calcium entry through voltage-gated L-type Ca^{2+} channels, because the effect persisted even when cardiomyocytes were incubated in Ca^{2+}-free/EGTA-containing resting solution or in the presence of nifedipine. The inhibition of IGF-1-dependent $[Ca^{2+}]_i$ increase by BAPTA-AM and thapsigargin indicate that Ca^{2+} was released from intracellular stores.

Confocal and epifluorescence microscopy images suggest that IGF-1 stimulates Ca^{2+} release from perinuclear regions, producing first a fast Ca^{2+} increase in the nucleus followed later by a cytosolic increase. Jaconi *et al.* (46) showed that

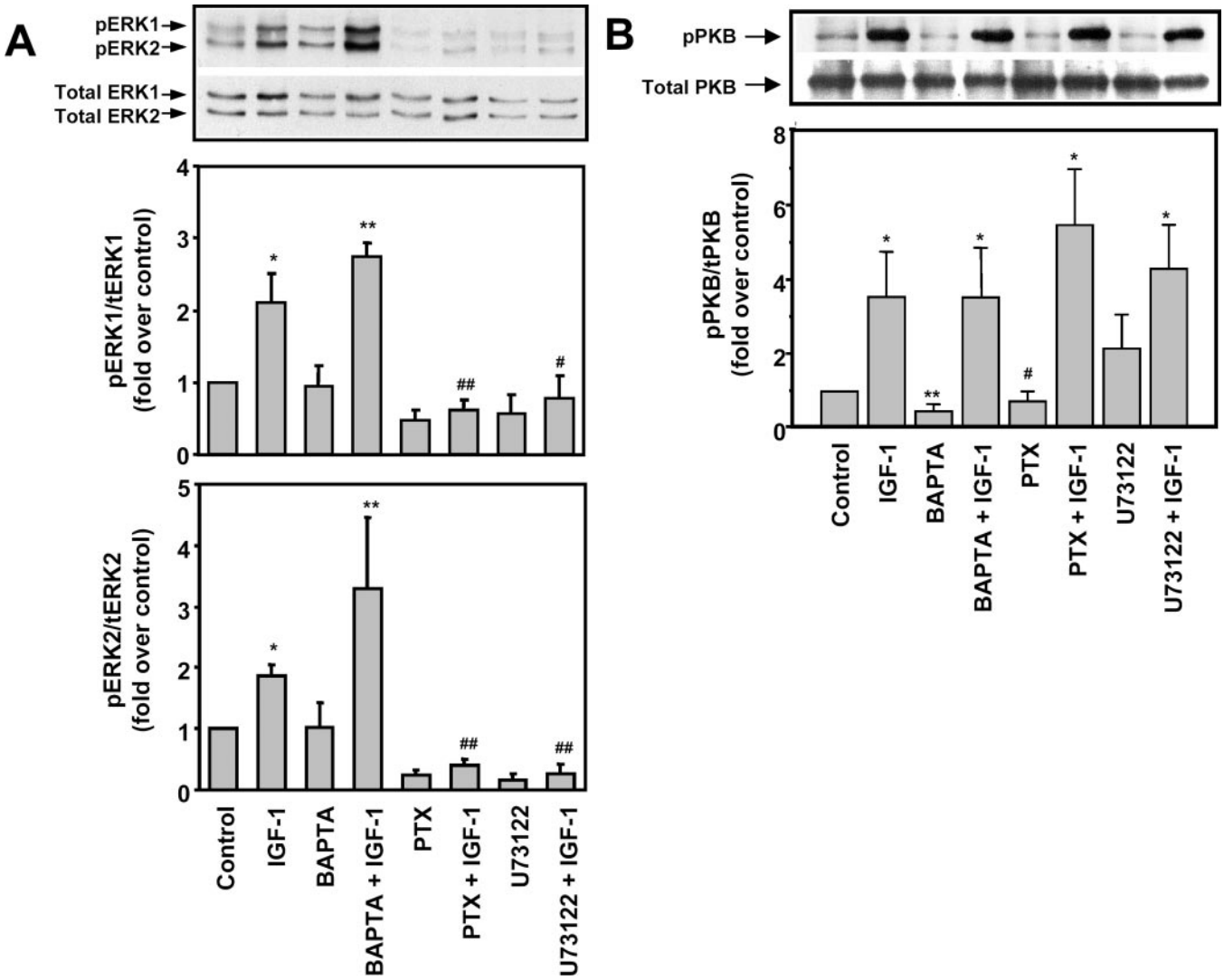

FIG. 10. **Effect of BAPTA, PTX, and phospholipase C inhibitor U73122 on the IGF-1-induced activation of ERK1, ERK2, and PKB.** Cultured rat cardiomyocytes, maintained in Ca^{2+}-free resting media, were preincubated with PTX (1 μg/ml) for 90 min or BAPTA-AM (100 μM) and U73122 (50 μM) for 30 min, and then stimulated with IGF-1 (1 nM) during 5 min. *A*, phosphorylated and total ERK1 and ERK2 ratio (*pERK/tERK*); and *B*, phosphorylated and total PKB ratio (*pPKB/tPKB*) were quantified from Western blots of total protein extracts as described under "Experimental Procedures." Values represent the average of at least three different experiments ± S.E. **, $p < 0.01$ and *, $p < 0.05$ *versus* basal; ##, $p < 0.01$ and #, $p < 0.05$ *versus* IGF-1.

adenosine-dependent $[Ca^{2+}]$ oscillations in cardiac myocytes are elicited by Ca^{2+} release from the perinuclear region, which also produce a fast increase of nuclear Ca^{2+} levels.

Cardiomyocytes stimulated with IGF-1 in the presence of extracellular Ca^{2+} exhibited a slower increase in $[Ca^{2+}]_i$ than that observed in the absence of extracellular Ca^{2+}. ROI analysis of fluorescence images revealed that external Ca^{2+} slowed down only the cytosolic but not the nuclear Ca^{2+} increase. As discussed below, differences in the time course of the IP_3 mass increase induced by IGF-1 addition with and without external Ca^{2+} could explain the differences in Ca^{2+} transient kinetics seen in both conditions.

Cardiomyocytes pretreated with ryanodine (20 μM) and stimulated with IGF-1 in the absence of extracellular Ca^{2+} exhibited a slower increase in $[Ca^{2+}]_i$ than that observed in the absence of ryanodine. ROI analysis of fluorescence images revealed that ryanodine, in analogy to the effect of extracellular Ca^{2+}, slowed down the cytosolic but not the nuclear Ca^{2+} increase. These results suggest that Ca^{2+} release through ryanodine receptors contributes to the fast cytosolic $[Ca^{2+}]$ increase but not to the nuclear Ca^{2+} increase produced by IGF-1 stimulation in the absence of extracellular Ca^{2+}. The ensemble of results suggests that at least two independent pathways for IGF-1-induced calcium release coexist in cardiac myocytes; release at the nuclear level is independent of both external calcium and ryanodine receptors. At the cytosolic level, on the other hand, a fast component of the calcium transient appears to be regulated by the presence of external calcium and also to partly depend on ryanodine receptor activation. A slow cytosolic component, not altered by ryanodine, also appears to be there.

The fact that different types of IP_3 receptors are expressed in cytosolic and perinuclear regions may explain the differences in calcium signaling kinetics between the two compartments. In fact, both affinity for IP_3 and calcium dependence for activation have been reported to differ between the different isoforms (47).

The effects of IP_3 inhibitors on both IGF-1-induced $[Ca^{2+}]_i$ transients and IP_3 mass increase strongly suggest a role for IP_3-regulated Ca^{2+} channels in eliciting these signals. The slower increase in IP_3 mass induced by IGF-1 in the presence of external Ca^{2+} could explain why the cytosolic Ca^{2+} increase was also slower in this condition. Different PLCs generate IP_3 in the heart (48–53). Some neurohumoral agonists, including

acetylcholine, endothelin, catecholamines, and prostaglandins (48–50) activate a G_q-dependent phospholipase Cβ (PLC-β). In contrast, purines or angiotensin II stimulate a tyrosine kinase-dependent PLC-γ (51, 52). PLC-δ has also been described in heart (53). Although all PLC isozymes require Ca^{2+} for activity, the PLC-δ type has the highest Ca^{2+} sensitivity, suggesting that it may be physiologically regulated by Ca^{2+} (54). A differential regulation of cardiac PLC isoforms by both IGF-1 and Ca^{2+} could explain the different kinetics for the IP_3 mass increase observed in the presence or absence of external Ca^{2+}. However, further studies are needed to clarify this point.

In cardiac muscle, some reports have also described the IP_3-dependent Ca^{2+} release. Thus, IP_3 is capable of inducing a slow release of calcium from vesicular preparations and of activating contraction in skinned ventricular rat muscle and chick heart preparations (55). Borgatta *et al.* (56) identified a low conductance, IP_3-sensitive, calcium release channel in sarcoplasmic reticulum vesicle preparations from canine heart. Consistently with the presence of an IP_3 signaling pathway in cardiac tissue, IP_3 receptors have also been described. Rat and ferret adult ventricular myocytes (57, 58) and rat adult atrial myocytes (59) express type 2 IP_3 receptors as their main isoforms. Both type 2 and type 3 IP_3 receptors were also identified in neonatal rat cardiomyocytes but with different intracellular localizations (46). Our results also described the presence of type 1 IP_3 receptor in neonatal rat cardiac myocytes. Western blot and immunocytochemical studies showed that type 1 and type 3 IP_3 receptors were mainly located in the nucleus, whereas type 2 IP_3 receptor was located almost exclusively in the cytosol. The participation of IP_3 receptors on IGF-1 action was established because both xestospongin C and 2-aminoethoxy diphenyl borate completely blocked the IGF-1-induced $[Ca^{2+}]_i$ increase. Moreover, differences in the cellular distribution of IP_3 receptor isoforms could explain in part the cellular compartmentalization of Ca^{2+} transients induced by IGF-1. The role of IP_3 receptors in cardiac myocytes is controversial, with suggestions that they play only a minor role during cardiac Ca^{2+} signaling or have a solely organelle-specific function (58). However, Lipp *et al.* (59) and Mackenzie *et al.* (60) showed that the type 2 IP_3 receptor regulates the arrhythmogenic potency of endothelin-1 in atrial myocytes and could modulate excitation-contraction coupling, respectively.

Participation of Other Signaling Cascades in IGF-1 Stimulation of Cultured Cardiac Myocytes—The IGF-1-induced increases in Ca^{2+} transients and IP_3 mass were both totally suppressed by pretreatment of rat cardiomyocytes with PTX, suggesting the involvement of a PTX-sensitive G protein in these responses. The IGF-1-induced Ca^{2+} transients were also reduced by the expression of βARK-ct, indicating that G$\beta\gamma$ subunits from the G_i protein are involved. Additionally, LY294002, a PI3K inhibitor, completely blocked the IGF-1-induced Ca^{2+} transients, indicating the participation of PI3K in the IGF-1 induced Ca^{2+} signaling pathway. Bony *et al.* (61) have described that PI3K-γ activation is a crucial step in the purinergic regulation of rat cardiomyocyte spontaneous Ca^{2+} spiking, and LY294002 treatment of these cells prevented tyrosine phosphorylation and membrane translocation of PLC-γ, as well as IP_3 generation on ATP-stimulated cells. Hong *et al.* (62) showed that in IGF-1-induced muscle differentiation, using H9c2 rat cardiac myoblasts as a model, there was activation of PLC-γ 1 via both PI3K-dependent and tyrosine kinase-dependent mechanisms. Furthermore, PLC-γ 1 activation was independent of PKB (62).

As indicated above, IGF-1 binding to the IGF-1 receptor activates PI3K through the involvement of IRS proteins (12, 63) in a G_i protein-independent mechanism (14). However, the

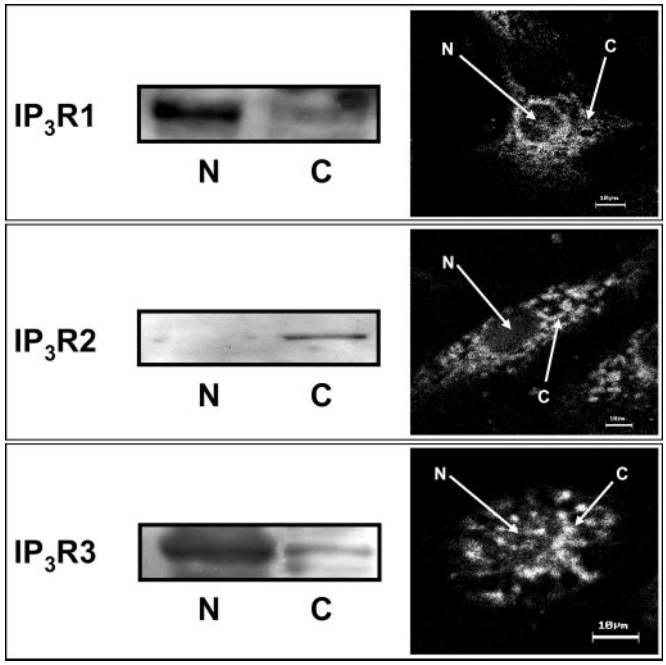

FIG. 11. **Subcellular distribution of IP_3 receptors in cultured cardiomyocytes.** Western blot analysis in nuclear (*N*) and cytosol (*C*) protein extracts (*left panels*) and immunocytochemistry studies (*right panels*) of type 1, type 2, and type 3 IP_3 receptors were performed as described under "Experimental Procedures." Figures are representative of three independent experiments with similar results.

Gβ_γ subunit of trimeric G_i proteins can activate PI3K-γ by direct interaction with two domains of the catalytic p110 subunit (64). Using a pressure load hypertrophy model, Prasad *et al.* (65) demonstrated that PI3K was activated in mice *in vivo* by a G$\beta\gamma$-dependent process. Therefore, IGF-1 could activate PI3K by a PTX-sensitive pathway through the G$\beta\gamma$ subunit of a G_i protein.

Recent reports in different cell types have proposed the involvement of the G_i protein but not of PI3K/PKB signaling pathways in IGF-1 receptor-dependent ERK activation (13–16). Our results also show that in cardiomyocytes IGF-1 receptor-dependent ERK activation required PTX-sensitive G protein. In contrast, IGF-1 receptor-dependent PKB activation was insensitive to PTX.

Pretreatment of rat cardiomyocytes with PD98059, a MEK inhibitor, did not block the IGF-1-induced Ca^{2+} transients, but modified its kinetics. Because cells were preincubated with PD98059 30 min before IGF-1 stimulation, this inhibitor could change basal ERK-dependent phosphorylation within the cells. This alteration could in turn change the observed Ca^{2+} transient kinetics. Moreover, the Ca^{2+} signaling inhibitor U73122, but not BAPTA, prevented IGF-1-dependent ERK activation. Taken together, these results suggest that the MEK-ERK signaling cascade was not necessary for IGF-1-dependent Ca^{2+} release, but intracellular Ca^{2+} increases may promote ERK phosphorylation. This observation agrees with previous findings in PC12 cells and chicken motor neurons; in these cells membrane depolarization activates the ERK signaling pathway through a Ca^{2+}/calmodulin-dependent mechanism that involves $p21^{ras}$ activation (66).

In summary (see Fig. 12), our results suggest that IGF-1 induces Ca^{2+} release by a sequential mechanism involving its binding to the IGF-1 receptor, activation of a PTX-sensitive G protein followed by G$\beta\gamma$ subunit-dependent activation of PI3K. This kinase, through indirect activation of PLC, would be responsible in turn for the IP_3 mass increase; finally the subsequent activation of IP_3 receptors in the perinuclear region

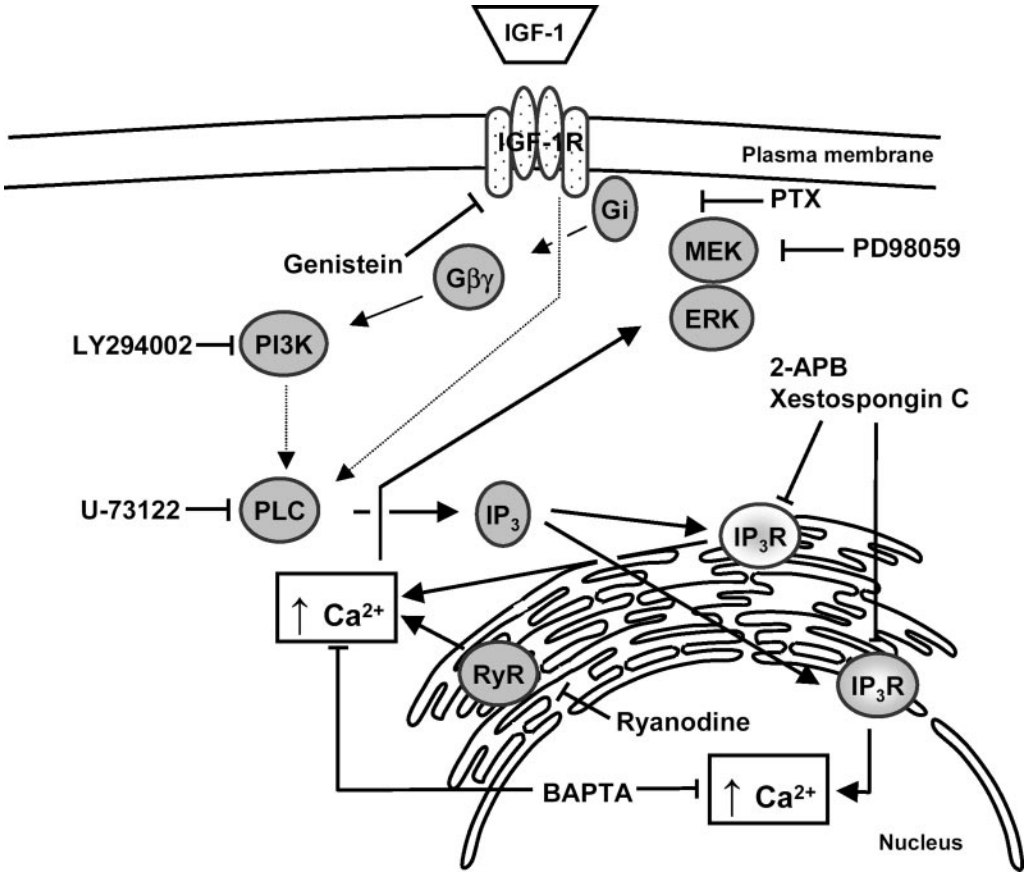

FIG. 12. **Proposed mechanism for the generation of Ca^{2+} transients by IGF-1 in cultured rat cardiomyocytes.** *RyR*, ryanodine receptor; *IP_3R*, IP_3 receptor (at least two different isoforms of IP_3R are considered).

would result in Ca^{2+} release from intracellular stores to the nucleus and the cytoplasm. IGF-1 activation of MEK-ERK is not directly implicated in Ca^{2+} release in cardiac myocytes. However, the basal ERK phosphorylation state is somehow involved in modulating $Ca^{2+}{}_i$ signaling kinetics.

Hypertrophy and IGF-1-dependent Calcium Increase—IGF-1 is a well known pro-hypertrophic hormone (3–5). Cardiac hypertrophy is an adaptive mechanism to enhance cardiac output in response to several cardiovascular disorders, including hypertension, myocardial infarction, vascular disease, and contractile abnormalities resulting from sarcomeric protein mutations (67). During the hypertrophic response, cardiac myocytes increase in size without undergoing cell division, assemble additional sarcomeres, and activate a fetal program of cardiac gene expression (68). Hypertrophic growth of cardiomyocytes is triggered by Ca^{2+}, acting as an important second messenger for diverse signals including angiotensin II, endothelin-1, α-adrenergic agents, and mechanical stretching (69). The pro-hypertrophic action of IGF-1 has been associated with the MEK-ERK signaling pathway (70). The effects of IGF-1 on $[Ca^{2+}]_i$ open the possibility of studying Ca^{2+} as a new potential second messenger of the IGF-1-induced signaling cascade to induce cardiac hypertrophy.

Acknowledgments—We thank Dr. W. J. Koch for the βARKct and EV adenovirus, Dr. Cecilia Hidalgo for critical reading of the manuscript, and Fidel Albornoz for technical assistance.

REFERENCES

1. Liu, J. L., Yakar, S., and LeRoith, D. (2000) *Endocrinology* **141,** 4436–4441
2. Engelmann, G. L., Boehm, K. D., Haskell, J. F., Khairallah, P. A., and Ilan, J. (1989) *Mol. Cell. Endocrinol.* **63,** 1–14
3. Ito, H., Hiroe, M., Hirata, Y., Tsujino, M., Adashi, S., Shichiri, M., Koyke, A., Nogami, A., and Marumo, F. (1993) *Circulation* **87,** 1715–1721
4. Duerr, R., Huang, S., Miraliakbar, H., Clark, R., Chien, K., and Ross, J. (1995) *J. Clin. Invest.* **95,** 619–627
5. Cittadini, A., Strömer, H., Hatz, S. E., Clark, R., Moses, A. C., Morgan, J. P., and Douglas, P. S. (1996) *Circulation* **93,** 800–809
6. Otani, H., Yamamura, T., Nakao, Y., Hattori, R., Kawaguchi, H., Osako, M., and Imamura, H. (2000) *J. Cardiovasc. Pharmacol.* **35,** 275–281
7. Buerke, M., Murohara, T., Skurk, C., Nuss, C., Tomaselli, K., and Lefer, A. M. (1995) *Proc. Natl. Acad. Sci. U. S. A.* **92,** 8031–8035
8. Li, Q., Li, B., Wang, X., Leri, A., Jana, K. P., Liu, Y., Kajstura, J., Baserga, R., and Anversa, P. (1997) *J. Clin. Invest.* **100,** 1991–1999
9. Fujio, Y., Nguyen, T., Wencker, D., Kitsis, R. N., and Walsh, K. (2000) *Circulation* **101,** 660–667
10. Ward, C. W., Garrett, T. P., McKern, N. M., Lou, M., Cosgrove, L. J., Sparrow, L. G., Frenkel, M. J., Hoyne, P. A., Elleman, T. C., Adams, T. E., Lovrecz, G. O., Lawrence, L. J., and Tulloch, P. A. (2001) *Mol. Pathol.* **54,** 125–132
11. Dupont, J., and LeRoith, D. (2001) *Horm. Res.* **55,** 22–26
12. Petley, T., Graff, K., Jiang, W., Yang, H., and Florini, J. (1999) *Horm. Metab. Res.* **31,** 70–76
13. Luttrell, L. M., van Biesen, T., Hawes, B. E., Koch, W. J., Touhara, K., and Lefkowitz, R. J. (1995) *J. Biol. Chem.* **270,** 16495–16498
14. Kuemmerle, J. F., and Murthy, K. S. (2001) *J. Biol. Chem.* **276,** 7187–7194
15. Dalle, S., Ricketts, W., Imamura, T., Vollenweider, P., and Olefsky, J. M. (2001) *J. Biol. Chem.* **276,** 15688–15695
16. Hallak, H., Seiler, A. E., Green, J. S., Ross, B. N., and Rubin, R. (2000) *J. Biol. Chem.* **275,** 2255–2258
17. Kojima, I., Matsunaga, H., Kurokawa, K., Ogata, E., and Nishimoto, I. (1988) *J. Biol. Chem.* **263,** 16561–16567
18. Kojima, I., Mogami, H., and Ogata, E. (1992) *Am. J. Physiol.* **262,** E307–E311
19. Geertz, R., Kiess, W., Kessler, U., Hoeflich, A., Tarnok, A., and Gercken, G. (1997) *Mol. Cell. Biochem.* **177,** 33–45
20. Poiraudeau, S., Lieberherr, M., Kergosie, N., and Corvol, M. T. (1997) *J. Cell. Biochem.* **64,** 414–422
21. Selinfreund, R. H., and Blair, L. A. (1994) *Mol. Pharmacol.* **45,** 1215–1220
22. Blair, L. A., and Marshall, J. (1997) *Neuron* **19,** 421–429
23. Kleppisch, T., Klinz, F. J., and Hescheler, J. (1992) *Brain Res.* **591,** 283–288
24. Chik, C. L., Li, B., Karpinski, E., and Ho, A. K. (1997) *Endocrinology* **138,** 2033–2042
25. Renganathan, M., Sonntag, W. E., and Delbono, O. (1997) *Biochem. Biophys. Res. Commun.* **235,** 784–789
26. Solem, M. L., and Thomas, A. P. (1998) *Biochem. Biophys. Res. Commun.* **252,** 151–155
27. Cittadini, A., Ishiguro, Y., Strömer, H., Spindler, M., Moses, A. C., Clark, R., Douglas, P. S., Ingwall, J. S., and Morgan, J. P. (1998) *Circ. Res.* **83,** 50–59
28. Freestone, N. S., Ribaric, S., and Mason, W. T. (1996) *Mol. Cell. Biochem.* **163–164,** 223–229
29. Foncea, R., Andersson, M., Ketterman, A., Blakesley, V., Sapag-Hagar, M.,

Sugden, P. H., LeRoith, D., and Lavandero, S. (1997) *J. Biol. Chem.* **272,** 19115–19124
30. Foncea, R., Gálvez, A., Pérez, V., Morales, M. P., Calixto, A., Meléndez, J., González-Jara, F., Díaz-Araya, G., Sapag-Hagar, M., Sugden, P. H., LeRoith, D., and Lavandero, S. (2000) *Biochem. Biophys. Res. Commun.* **273,** 736–744
31. United States National Institutes of Health (1985) *Guide for the Care and Use of Laboratory Animals*, National Institutes of Health Publication 85-23
32. Takahashi, T., Fukuda, K., Pan, J., Kodama, H., Sano, M., Makino, S., Kato, T., Manabe, T., and Ogawa, S. (1999) *Circ. Res.* **85,** 884–891
33. Shah, A. S., White, D. C., Emani, S., Kypson, A. P., Lilly, R. E., Wilson, K., Glower, D. D., Lefkowitz, R. J., and Koch, W. J. (2001) *Circulation* **103,** 1311–1316
34. Koch, W. J., Hawes, B. E., Inglese, J., Luttrell, L. M., and Lefkowitz, R. J. (1994) *J. Biol. Chem.* **269,** 6193–6197
35. Liberona, J. L., Powell, J. A., Shenoi, S., Petherbridge, L., Caviedes, R., and Jaimovich, E. (1998) *Muscle Nerve* **21,** 902–909
36. Lowry, O. H., Rosebrough, N. J., Farr, A. L., and Randall, R. J. (1951) *J. Biol. Chem.* **193,** 265–275
37. Minta, A., Kao, J. P., and Tsien, R. Y. (1989) *J. Biol. Chem.* **264,** 8171–8178
38. Castleman, K. (1989) *Digital Image Processing*, Prentice-Hall, Englewood Cliffs, NJ
39. Estrada, M., Liberona, J. L., Miranda, M., and Jaimovich, E. (2000) *Am. J. Physiol.* **279,** E132–E139
40. Schreiber, E., Matthias, P., Müller, M., and Schaffer, W. (1989) *Nucleic Acids Res.* **17,** 6413–6422
41. Hilenski, L. L., Terracio, L., and Borg, T. K. (1991) *Cell Tissue Res.* **264,** 577–587
42. Vlcek, S., Dechat, T., and Foisner, R. (2001) *Cell. Mol. Life Sci.* **58,** 1758–1765
43. Yano, K., and Zarain-Herzberg, A. (1994) *Mol. Cell. Biochem.* **135,** 61–70
44. Estrada, M., Cardenas, C., Liberona, J. L., Carrasco, M. A., Mignery, G. A., Allen, P. D., and Jaimovich, E. (2001) *J. Biol. Chem.* **276,** 22868–22874
45. Koch, W. J., Hawes, B. E., Allen, L. F., and Lefkowitz, R. J. (1994) *Proc. Natl. Acad. Sci. U. S. A.* **91,** 12706–12710
46. Jaconi, M., Bony, C., Richards, S. M., Terzic, A., Arnaudeau, S., Vassort, G., and Pucéat, M. (2000) *Mol. Biol. Cell* **11,** 1845–1858
47. Leite, M. F., Thrower, E. C., Echevarria, W., Koulen, P., Hirata, K., Bennett, A. M., Ehrlich, B. E., and Nathanson, M. H. (2003) *Proc. Natl. Acad. Sci. U. S. A.* **100,** 2975–2980
48. Brown, J. H., and Jones, L. G. (1986) in *Phosphoinositides and Receptor Mechanisms* (Putney, J. W., ed) pp. 245–270, Alan R. Liss, Inc., New York
49. Hilal-Dandan, R., Urasawa, K., and Brunton, L. L. (1992) *J. Biol. Chem.* **267,** 10620–10624
50. Adams, J. W., Sah, V. P., Henderson, S. A., and Brown, J. H. (1998) *Circ. Res.* **83,** 167–178
51. Puceat, M., and Vassort, G. (1996) *Biochem. J.* **318,** 723–728
52. Goutsouliak, V., and Rabkin, S. W. (1997) *Cell. Signalling* **9,** 505–512
53. Lee, W. K., Kim, J. K., Seo, M. S., Cha, J. H., Lee, K. J., Rha, H. K., Min, D. S., Jo, Y. H., and Lee, K. H. (1999) *Biochem. Biophys. Res. Commun.* **261,** 393–399
54. Rhee, S. G., and Bae, Y. S. (1997) *J. Biol. Chem.* **272,** 15045–15048
55. Hirata, M., Suematus, E., Hashimoto, T., Hamachi, T., and Koga, T. (1984) *Biochem. J.* **223,** 229–236
56. Borgatta, L., Watras, J., Katz, A. M., and Ehrlich, B. E. (1991) *Proc. Natl. Acad. Sci. U. S. A.* **88,** 2486–2489
57. Perez, P. J., Ramos-Franco, J., Fill, M., and Mignery, G. A. (1997) *J. Biol. Chem.* **272,** 23961–23969
58. Marks, A. R. (2000) *Circ. Res.* **87,** 8–11
59. Lipp, P., Laine, M., Tovey, S. C., Burrell, K. M., Berridge, M. J., Li, W., and Bootman, M. D. (2000) *Curr. Biol.* **10,** 939–942
60. Mackenzie, L., Bootman, M. D., Laine, M., Berridge, M. J., Thuring, J., Holmes, A., Li, W. H., and Lipp, P. (2002) *J. Physiol.* **541,** 395–409
61. Bony, C., Roche, S., Shuichi, U., Sasaki, T., Crackower, M. A., Penninger J., Mano, H., and Pucéat, M. (2001) *J. Cell Biol.* **152,** 717–727
62. Hong, F., Moon, K., Kim, S. S., Kim, Y. S., Choi, Y. K., Bae, Y. S., Suh, P. G., Ryu, S. H., Choi, E., Ha, J., and Kim, S. S. (2001) *Biochem. Biophys. Res. Commun.* **282,** 816–822
63. Butler, A. A., Yakar, S., Gewolb, I. H., Karas, M., Okubo, Y., and LeRoith, D. (1998) *Comp. Biochem. Physiol. B* **121,** 19–26
64. Leopoldt, D., Hanck, T., Exner, T., Maier, U., Wetzker, R., and Nurnberg, B. (1998) *J. Biol. Chem.* **273,** 7024–7029
65. Prasad, S. V. N., Esposito, G., Mao, L., Koch, W. J., and Rockman, H. A. (2000) *J. Biol. Chem.* **275,** 4693–4698
66. Egea, J., Espinet, C., and Comella, J. X. (1999) *J. Biol. Chem.* **274,** 75–85
67. Hunter, J. J., and Chien, K. R. (1999) *N. Engl. J. Med.* **341,** 1276–1283
68. Frey, N., McKinsey, T. A., and Olson, E. N. (2000) *Nature Med.* **6,** 1221–1227
69. McKinsey, T. A., and Olson, E. N. (1999) *Curr. Opin. Genet. Dev.* **9,** 267–274
70. Lavandero, S., Foncea, R., Pérez, V., and Sapag-Hagar, M. (1998) *FEBS Lett.* **422,** 193–196